Experimental Data for Uncertainty Quantification

MI Friswell, JE Coote, MJ Terrell, S Adhikari, JR Fonseca[¥], NAJ Lieven

Department of Aerospace Engineering, University of Bristol, Bristol BS8 1TR, UK
[¥] School of Engineering, University of Wales Swansea, Swansea SA2 8PP, UK.

ABSTRACT

The propagation of parameter uncertainty through a model to obtain the uncertain vibration response is becoming more practical for industrial scale finite element models due to the increase in computing power available. In some cases the parametric uncertainty may be measured directly, for example the thickness of a panel. However the parameters for joint models (for example) must be estimated from measurements using the techniques of finite element model updating. In these cases the techniques of model updating must be extended to allow for uncertainty quantification from a series of measurements on nominally identically structures. The validation of these methods requires laboratory experiments where the uncertain parameter is measured directly and also estimated by updating. This paper outlines the results of experiments that may be used for this purpose, namely a moving mass on a free-free beam and a copper pipe with uncertain internal pressure. The data from these experiments will be freely available on the associated website at Bristol.

1. INTRODUCTION

The propagation of uncertainty in material or geometrical parameters through a finite element model to determine the uncertainty in the response has become a valuable and popular technique. Examples of the use of this approach range from robust design to reliability analysis, and computer code is available for stochastic finite element analysis and uncertainty propagation (examples of the latter are NESSUS and ST-ORM). These techniques work extremely well and give great insight into the robustness of structures. However all of these approaches rely on knowledge of the parameter uncertainty. For many parameters, such as panel thicknesses, direct measurement may be used to get the description of the uncertainty in terms of a probably density function. Tolerances may be used to give some insight into the variance for probabilistic approaches or the bounds for possiblistic approaches. However, direct measurement of many parameters is not possible. For example, the model of many joints is uncertain, but the nature of the modelling errors means that equivalent models must be used, based on generic elements, geometric parameters, or other techniques [1,2]. The uncertainty in the parameters must be obtained from measurements, using inverse methods [3, 4]. This paper describes two experiments that may be used to test methods of uncertainty quantification. The difference between this data and previous experimental data is that the tests are closely controlled and the parametric uncertainty is measured. This allows the identified uncertainty from model updating to be compared to the independently measured parameters.

The experimental data are available on the website http://www.aer.bris.ac.uk/research/uncertainty/.

2. FREE-FREE BEAM EXAMPLE

2.1. Experimental Setup

A beam of length 1 m and made from bright mild steel was suspended using flexible supports to simulate free-free conditions. A small mass (magnet) was attached to the beam and its position was varied using a normal distribution with mean, μ, of 800 mm and standard deviation, σ, of 30 mm. 50 mass positions were sampled from this distribution. The experimental setup is illustrated schematically in Figure 2.1. The mass properties and dimensions for the components are given in Table 2.1.

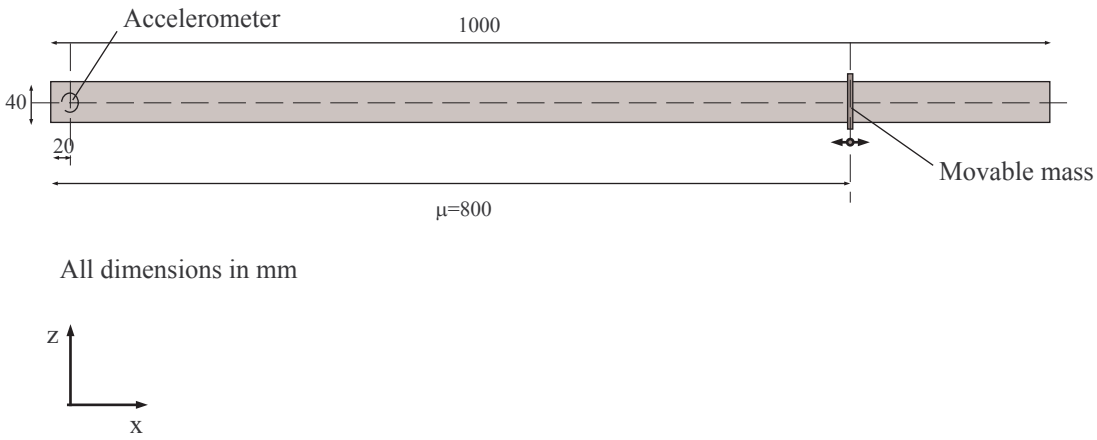

Figure 2.1. Experimental setup for the free-free beam.

Component	Mass (g)	X (mm)	Y (mm)	Z (mm)
Beam	1561	1000	40	5
Mass (Magnet)	47	5	50	25
Accelerometer	6			

Table 2.1. Component masses and dimensions for the beam example.

2.2. Test Procedure

For each test the centreline of the mass was aligned with the relevant position along the beam. The thinnest edge of the mass was placed in contact with the beam to minimise any stiffening effects. Impact excitation was used, and the average of three runs was taken at each mass location. The response was measured with a PCB Model 333M07 accelerometer located at 20 mm from the beam end, and excited by a PCB impact hammer with the impact location at 417 mm from the accelerometer end. The data acquisition and analysis performed using an LMS Test.Lab system with a bandwidth of 512 Hz and 4096 frequency lines and an exponential response window. The first three natural frequencies were estimated from the FRFs using time domain parameter extraction.

2.3. Results

Figure 2.2 shows the frequency response functions up to 200 Hz at all mass positions. This frequency range covers the first three bending modes of the beam. A rigid body mode between 2 and 3 Hz is clearly visible. Notice that the natural frequency of the first mode changes very little with the mass position, whereas modes 2 and 3 change significantly. For comparison a free-free beam model was created using 50 elements. Figure 2.3 compares the experimental and numerical FRFs when the moving mass was at its mean position of 800 mm from the accelerometer end. Clearly the model is reasonably close and the discrepancies arise from small differences in natural frequency caused by small differences in the flexural rigidity, *EI*, that are likely to be within the measurement tolerances of the beam thickness. The other significant difference is that the numerical model was undamped.

Figure 2.4 shows the first two natural frequencies as a function of the position of the mass. For comparison the numerical results are also shown. The natural frequencies change smoothly with mass position and, apart from the offset due to the modelling error described above, the experimental and numerical result corresponded closely. This figure also highlights the mass positions used for the experiments, which were taken from a normal distribution.

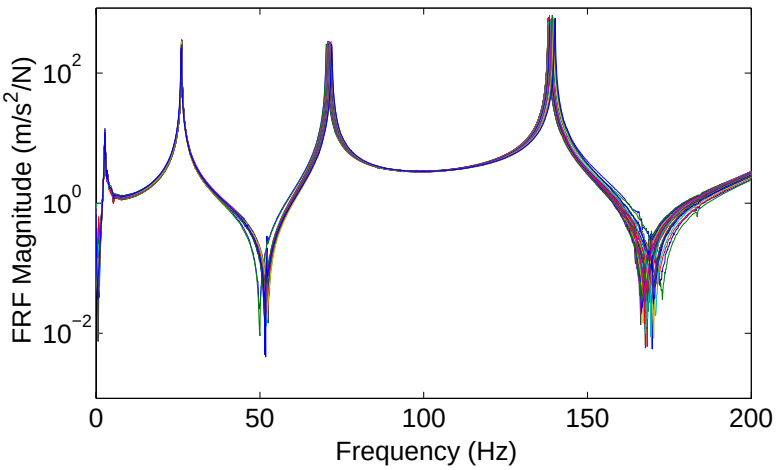

Figure 2.2. Experimental FRFs for all mass positions for the beam example.

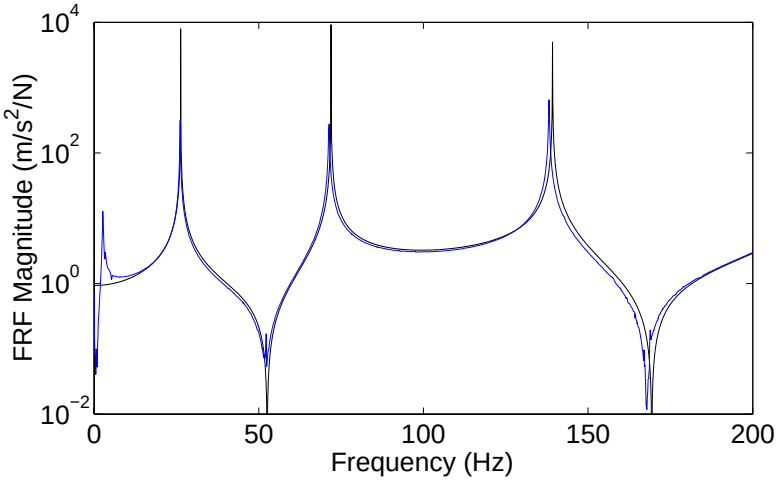

Figure 2.3. Comparison of experimental and numerical FRFs for the mean mass position for the beam example.

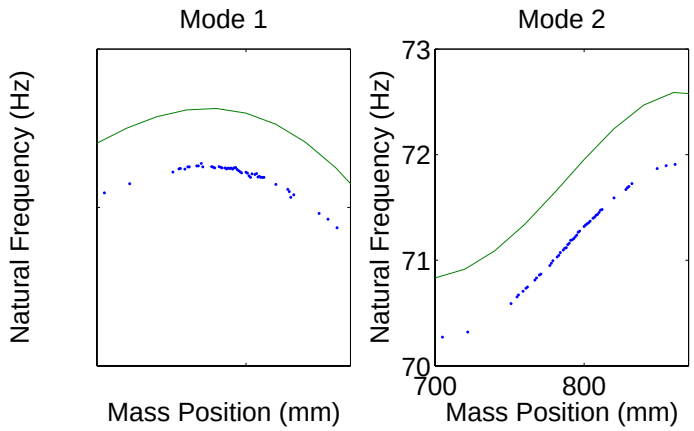

Figure 2.4. The variation of natural frequency with mass position for the beam example (the blue dots denote experimental data points).

3. PIPE EXAMPLE

3.1. Experimental Setup

The test rig has been designed for simplicity and ease of replication and modelling. It consists of a length of copper piping as used for domestic plumbing, with both ends terminated by a standard brass stop end compression fitting. To ensure that the joints are airtight, jointing compound was applied to the thread and olive, and each nut was tightened by a quarter-turn beyond initial finger-tight resistance. To enable pressurisation, a hole was drilled and tapped into one of the endpieces to securely admit a bicycle valve, as shown in Figure 3.1. The copper pipe conforms to the BS EN 1057 standard, and has 22 mm outside diameter, 0.9 mm wall thickness, length 2012 mm, and is annealed to the 'halfhard' temper (R250) with nominal tensile strength at 250 MPa and a maximum working pressure of 740 psi (51 bar). An E-shock M-Blaster bicycle pump with integral digital pressure meter (to nearest ±0.5 psi) was used. Table 3.1 provides the component masses as measured.

Before dynamic measurements began, two pressure tests examined the integrity of the end fittings and the quality of the pressure seals. The pipe was 9/10ths filled with water, and the stop ends fitted. It maintained a pressure of 300 psi without any measureable drop over a period of 30 hours. The water was then released, the pipe dried, and a further pressure test was carried out at 300 psi while filled with air. Again, no pressure drop was measurable, and no leaks were seen when submerging either end in a bucket of water.

3.2. Test Procedure

The overall test arrangement is shown in Figure 3.2. While the pipe was unpressurised, it was clamped at both ends on the endcaps so as not to compress the pipe section, as shown in Figure 3.3. A shaker was attached to the pipe via an aluminium pushrod to a PCB force transducer bonded by J. B. Weld epoxy adhesive to the pipe surface at a distance of 315 mm from the inner end of the valveless stop end fitting (Figure 3.4). The transducer signal was conditioned by a Kistler unit with a gain of 20 and low-pass filter at 30 kHz, and was then further filtered by a multichannel Kemo unit; low-pass at 10 kHz, and high-pass at 0.1 Hz. Finally, the analyser applied additional lowpass and highpass filtering at the limits of each relevant frequency range of testing. Horizontal translational response was measured by an Ometron scanning laser doppler vibrometer at a point 582 mm inboard of the same stop end fitting, and filtered likewise by the Kemo unit.

In the test, the response at a single point was recorded at 50 pressures sampled from the normal distribution with mean 100 psi and standard deviation of 30 psi; pressures were rounded to the nearest psi, and multiple occurrences were measured singly. To establish repeatability of measurements, the lowest pressures were remeasured for comparison at the end of testing. In both tests, the measurements were taken in a single sitting with no significant temperature variations. A Bruel & Kjaer analyser was used to calculate the transfer functions. The frequency range was traversed in 800 Hz segments with a frequency resolution of 1 Hz, and 20 Hanning-windowed linear averages were taken in each case.

Component	Mass (g)
Copper pipe	1047.8
End stop cap	35.1
End stop nut	31.6
End stop olive	4.3
Jointing paste applied to each end	1 (estimated)

Table 3.1. Component masses for pipe example

Figure 3.1. Pipe end stop fitted with valve.

Figure 3.3. Clamp arrangement for pipe.

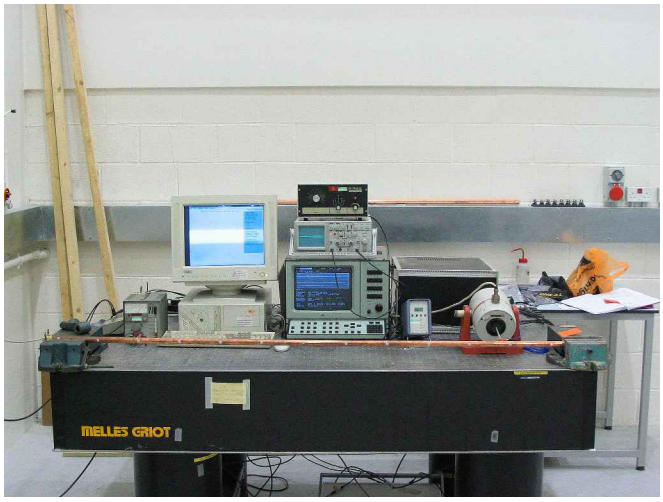

Figure 3.2. Pipe under test.

Figure 3.4. Shaker attachment for pipe example.

3.3. Results

Figure 3.5 shows the pipe frequency responses at all tested pressures, over the full frequency range of 0-7.2 kHz. The lower part of the frequency range (Figure 3.6) shows little variation with pressure as would be expected, whereas significant shifts occur in the higher ranges (Figure 3.7). The frequency shift of the peaks with pressure is more clearly shown in Figure 3.8, with an interesting increase in sensitivity to pressure at 4 kHz and above. Although stress-stiffening would be expected to increase natural frequencies, this is not the case with all resonances, with several decreasing. In some regions of the spectrum, the modal uncertainty exceeds the modal spacing, as shown for 4.1-4.3 kHz in Figure 3.9.

Figure 3.10 shows two FRFs taken at the same pressure at the beginning and end of testing, demonstrating the repeatability of the procedure.

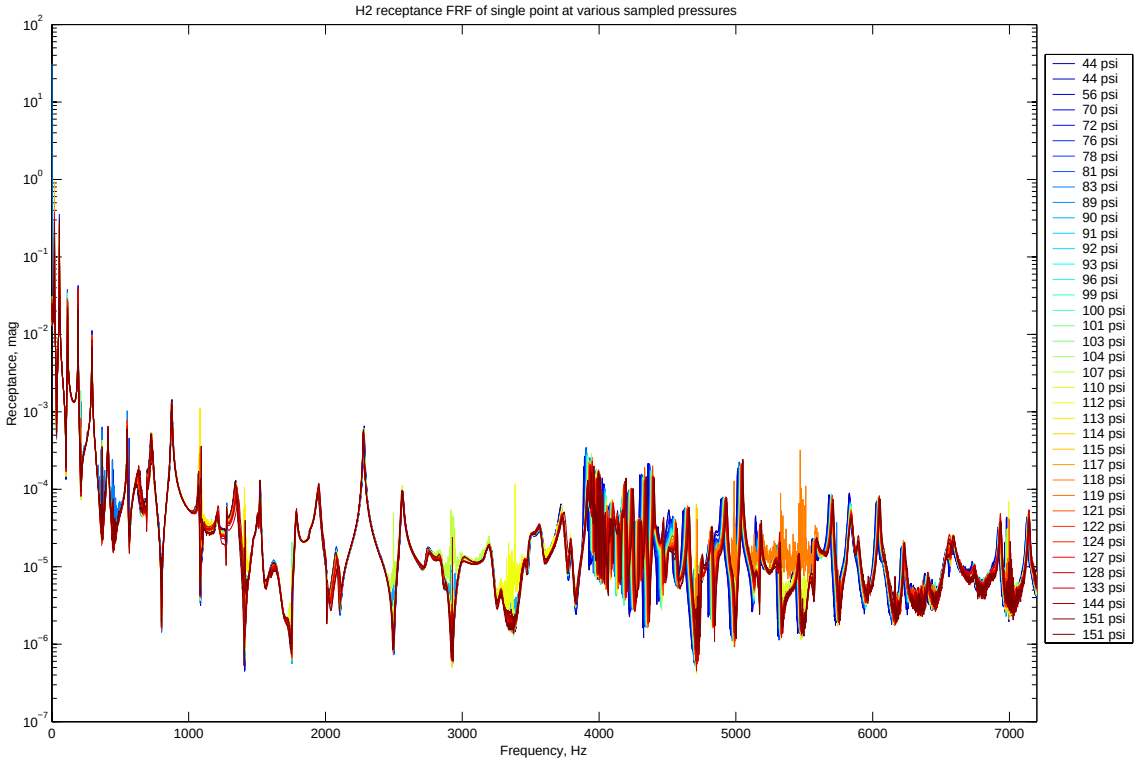

Figure 3.5. Pipe frequency response at all sampled pressures.

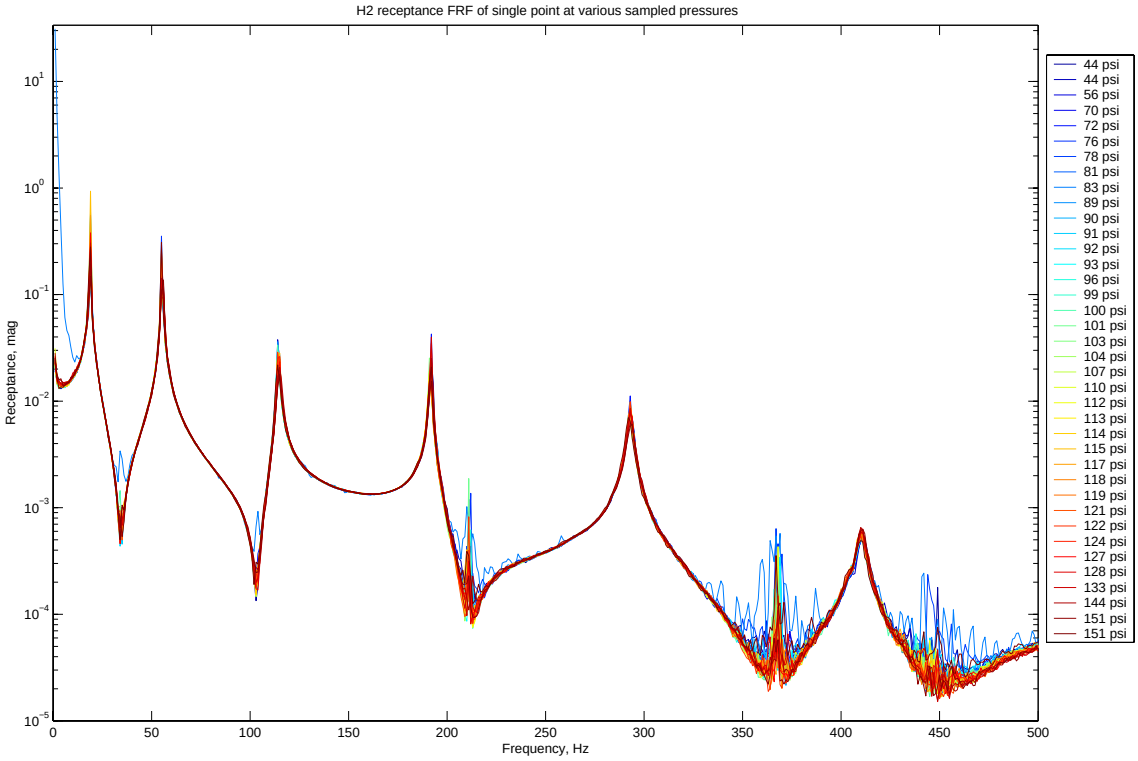

Figure 3.6. Pipe frequency response for all pressures, 0-500 Hz.

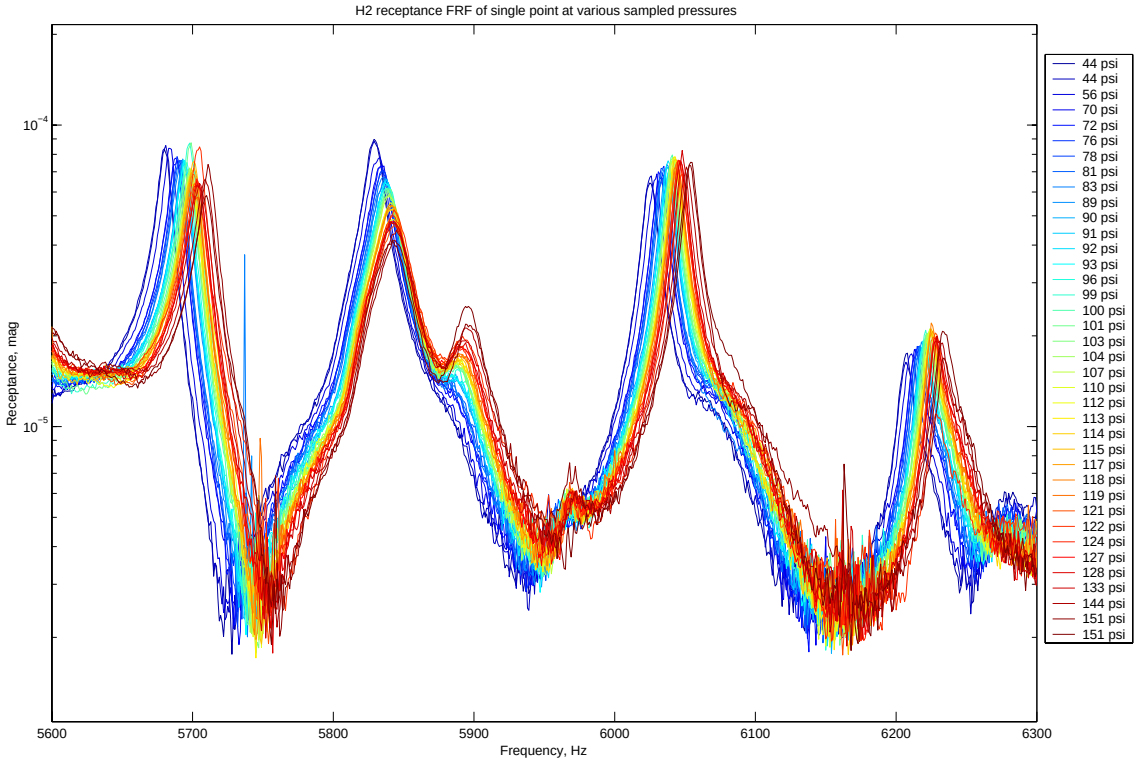

Figure 3.7. Pipe frequency response at all sampled pressures, 5600-6300 Hz.

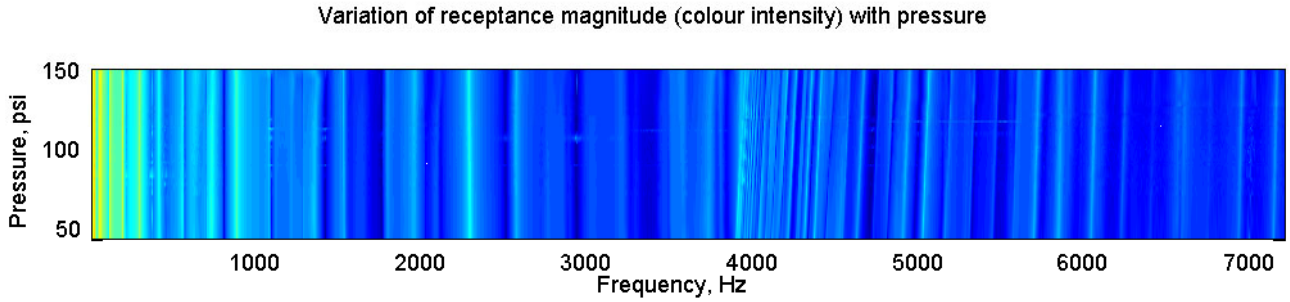

Figure 3.8. Frequency variation with pressure for the pipe example.

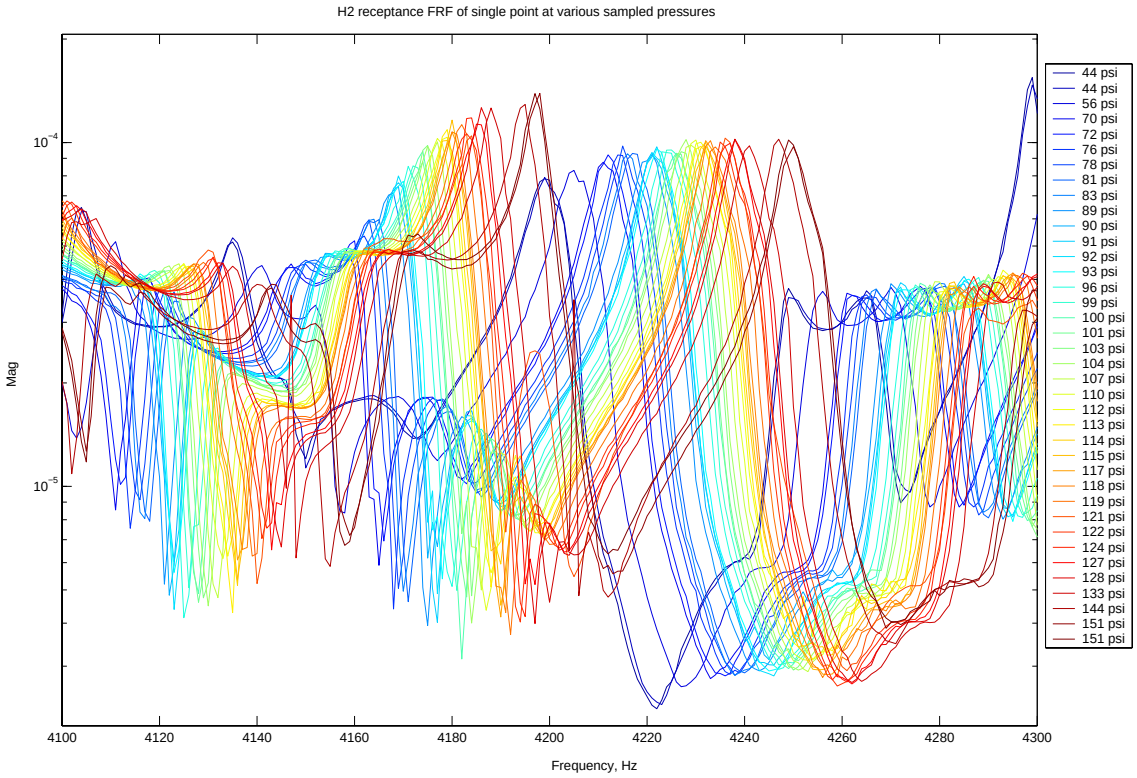

Figure 3.9. Pipe frequency response at all sampled pressures, 4.1-4.3 kHz.

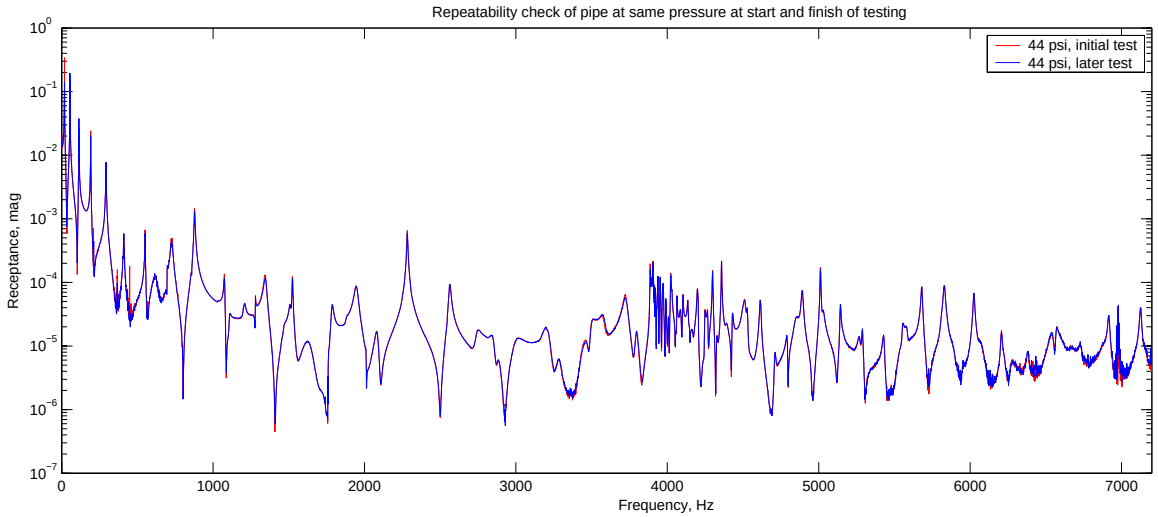

Figure 3.10. Repeatability check of FRF at start and finish of testing..

CONCLUSIONS

This paper has described two experiments that may be used to study methods to quantify uncertainty in the dynamics of structures. The free-free beam is very easy to model and the results of a 50 element model were described in this paper. The model did contain a systematic error that could be reduced by updating the beam stiffness, *EI*, as well as the mass position. Given that the first three natural frequencies have been estimated, this

example is easy to use to test uncertainty quantification algorithms. The pipe example is more complex, since the frequency range considered is much wider. The modal density is much higher, and in certain regions the uncertainty in natural frequency is greater than the spacing between natural frequencies. In this case quantifying uncertainty using natural frequencies is very difficult because mode shape pairing breaks down.

The FRF data, and natural frequency data for the beam example, may be downloaded from

http://www.aer.bris.ac.uk/research/uncertainty/.

ACKNOWLEDGEMENTS

The authors acknowledge the support of the Engineering and Physical Sciences Research Council (United Kingdom) through grant GR/R34936. Friswell acknowledges the support of a Royal Society-Wolfson Research Merit Award. Foncesa acknowledges the support of the Portuguese Foundation for Science and Technology through the scholarship SFRH/BD/7065/2001.

REFERENCES

1. Friswell, M.I., Mottershead, J.E. & Ahmadian, H., Finite Element Model Updating using Experimental Test Data: Parameterisation and Regularisation, *Transactions of the Royal Society of London, Series A: Mathematical, Physical and Engineering Sciences*, special issue on Experimental Modal Analysis, Vol. 359, pp. 169-186, 2001.
2. Mottershead, J.E., Friswell, M.I., Ng, G.H.T. & Brandon, J.A., Geometric Parameters for Finite Element Model Updating of Joints and Constraints, *Mechanical Systems and Signal Processing*, Vol. 10, No. 2, pp. 171-182, 1996.
3. Fonseca, J.R., Friswell, M.I., Mottershead, J.E. & Lees, A.W., Uncertainty Identification by the Maximum Likelihood Method, Special Issue of the *Journal of Sound and Vibration* on Uncertainty, in review.
4. Mares, C., Mottershead, J.E. & Friswell, M.I., Stochastic Model Updating of a Spot Welded Structure, *ISMA 2004*, Leuven, Belgium, 1885-1898, 2004.